Incremental induction of NMDAR-STP and NMDAR-LTP in the CA1 area of ventral hippocampal slices relies on graded activation of discrete NMDA receptors

Rachael Ingram[1], Rasa Volianskis[2,3], John Georgiou[2,4], David E Jane[5], Adina T. Michael-Titus[1], Graham L Collingridge[2,3,4] and Arturas Volianskis[1,6]

Affiliations
[1]Centre for Neuroscience, Surgery and Trauma, Blizard Institute, Barts and The London School of Medicine and Dentistry, Queen Mary University of London, London, UK
[2]Lunenfeld-Tanenbaum Research Institute, Mount Sinai Hospital, Sinai Health System, Toronto, ON, Canada
[3]Department of Physiology, University of Toronto, Toronto, ON, Canada
[4]TANZ Centre for Research in Neurodegenerative Diseases, University of Toronto, Toronto, ON, Canada
[5]Hello Bio Limited, Cabot Park, Avonmouth, Bristol, UK
[6]School of Biosciences, Cardiff University, Museum Avenue, Cardiff, UK

Corresponding Author
[6]Dr. Arturas Volianskis;
School of Biosciences, Cardiff University
Museum Avenue,
Cardiff, CF10 3AX, UK
Email: VolianskisA@cardiff.ac.uk

ORCID iDs:
R.I., 0000-0001-5300-4337
R.V., 0000-0002-1447-4878,
J.G., 0000-0003-4503-6384
A.T.M-T., 0000-0002-2961-6015
G.L.C., 0000-0002-9572-5359
A.V., 0000-0002-2047-8269

Keywords
Short-term potentiation (STP), Long-term potentiation (LTP), NMDA receptor (NMDAR), Ventral hippocampus, Dorsal hippocampus, Synaptic plasticity

Summary (198 words)

N-methyl-D-aspartate receptor (NMDAR)-dependent short- and long-term types of potentiation (STP and LTP, respectively) are frequently studied in the CA1 area of dorsal hippocampal slices (DHS). Far less is known about the NMDAR-dependence of STP and LTP in ventral hippocampal slices (VHS), where both types of potentiation are smaller in their magnitude than in the DHS. Here, we first briefly review our knowledge about the NMDAR-dependence of STP and LTP, and some other forms of synaptic plasticity. We then show in new experiments, that the decay of NMDAR-STP in VHS, similar to dorsal hippocampal NMDAR-STP, is not time- but activity-dependent. We also demonstrate that the induction of

submaximal levels of NMDAR-STP and NMDAR-LTP in VHS differs from the induction of saturated levels of plasticity in terms of their sensitivity to subunit-preferring NMDAR antagonists. These data suggest that activation of distinct NMDAR subtypes in a population of neurons results in an incremental increase in the induction of different phases of potentiation with changing sensitivity to pharmacological agents. Differences in pharmacological sensitivity, which arise due to differences in the levels of agonist-evoked biological response, might explain the disparity of the results concerning NMDAR subunit involvement in the induction of NMDAR-dependent plasticity.

Introduction

Different NMDA receptor dependent forms of synaptic plasticity: STP, LTP and LTD

Activity-dependent potentiation and depression of synaptic transmission is thought to underlie encoding of memories in the brain, and a variety of distinct types of synaptic plasticity have been described (1). Different forms of synaptic plasticity have been classified in a number of ways: e.g., (a) on the basis of their duration (2-4), (b) neurotransmitter systems and ion channels that contribute to their induction (5-7), or (c) second messenger systems that contribute to their expression and maintenance (3, 4, 6-8).

N-methyl-D-aspartate receptor (NMDAR)-dependent forms of synaptic plasticity, which include short-term potentiation (STP), long-term potentiation (LTP) and long-term depression (LTD), are some of the most frequently studied types of synaptic plasticity (1, 5, 9). STP, LTP and LTD rely on activation of NMDARs during their induction and have relatively long-lasting effects on the strength of synaptic transmission (> 30 min to years); making them attractive physiological candidates for the storage of memories (2, 5, 10). During the 50 years since the discovery of LTP (11, 12), LTP and LTD have attracted a lot of research attention, establishing themselves as putative correlates of long-term memory (10, 13). NMDAR-dependent STP (NMDAR-STP) has attracted less experimental interest than LTP and LTD, with some significant confusion in the literature.

The muddle about STP

A lot of the mix-up with regards to NMDAR-STP comes from the fact that some other forms of synaptic plasticity, such as paired-pulse facilitation (PPF), frequency facilitation (FF) and post-tetanic potentiation (PTP) are known under the umbrella term of "short-term plasticity" (4), with the unfortunate consequence of sharing the acronym "STP" with NMDAR-STP. PPF, FF and PTP are shorter-lasting (milliseconds, seconds or a few minutes) than NMDAR-STP (minutes to hours) and importantly, do not require NMDAR involvement for

their induction (4, 14-16). The phenomena of short-term plasticity may be involved in reverberating (or persistent) activity and working memory formation (17-22), somewhat similarly to NMDAR-STP, which is also thought to be involved in shorter-lasting memories when compared to LTP (23-25).

Adding to the confusion about the acronym is the fact that the differentiation of NMDAR-dependent STP (short-term potentiation) from NMDAR-independent STP (short-term plasticity) is a fairly recent development. Indeed, prior to the 1983 discovery of the role of NMDARs in LTP (26), most of the exponentially decaying potentiation phenomena, which can be observed at both the neuromuscular junction and at central synapses, were known as PTP (4, 20, 27, 28) - albeit with some exceptions e.g. (29). The separation of NMDAR-STP from PTP became more widely accepted after the 1993 review by Bliss and Collingridge, which divided plasticity into NMDAR-dependent and -independent types (1). It was much later that it was shown that NMDAR-STP and PTP are fundamentally different: (a) PTP in hippocampal synapses decays within ~ 2 min, whilst NMDAR-STP lasts ~20 min or more in most of experiments (23, 30), (b) PTP is independent of CAMKII, whilst NMDAR-STP has been shown to depend on CAMKII (30, 31), (c) the decay of PTP is time-dependent (23, 32), whilst NMDAR-STP decays in response to presynaptic activation - it is actively de-potentiated by stimulation (23, 33). Indeed, NMDAR-STP appears to be more similar to NMDAR-LTP than to the NMDAR-independent types of synaptic plasticity and therefore, due to its transiently-decaying nature, NMDAR-STP has been termed transient-LTP (t-LTP, (23)). However, the field did not agree with this change of the name and the muddle with the nomenclature continues unresolved. To avoid any further ambiguity, throughout the rest of this paper, we will refer to short-term potentiation as NMDAR-STP, in-contrast to the NMDAR-independent PTP and other NMDAR-independent forms of short-term plasticity. We will refer to NMDAR-dependent LTP, as LTP.

NMDAR-STP and LTP in the CA1 area of the Schaffer-collaterals in the hippocampus

NMDAR-STP and LTP are frequently co-induced at hippocampal synapses (Fig 1A, (23)), but they can also be induced independently of each other (29, 34-36). In contrast to LTP, which shifts the level of synaptic transmission towards potentiation in a static fashion (37, 38), NMDAR-STP is dynamic (24). Thus, NMDAR-STP modulates the synaptic frequency response (24), similarly to presynaptic forms of LTP (39-41), whilst post-synaptic LTP preserves the fidelity of the response, and amplifies neural transmission (37, 38). NMDAR-

STP increases during brief high-frequency bursts of activity and declines exponentially in response to infrequent synaptic activation either to baseline or to a sustained level of LTP (Fig 1A, (23, 27, 29, 42)). The rate of NMDAR-STP decay is directly related to the number of de-potentiating stimuli, such that NMDAR-STP decays faster in experiments with more frequent afferent stimulation than with slower stimulation (23, 27, 29). Thus, during periods of synaptic inactivity following the induction, the level of NMDAR-STP is "stored" in synapses, providing temporal stability in synaptic strength (Fig 1B, see also (33)). Storage of NMDAR-STP during periods of synaptic inactivity has been demonstrated for up to 6 hours in hippocampal slices (23), making it an attractive mechanism for storage of such memories that can neither be sustained by a reverberatory trace nor by a semi-permanent structural alteration (21). Differently from LTP, which saturates after ~ 2 s of theta-burst stimulation (43), NMDAR-STP can be repeatedly re-induced and de-potentiated under the baseline conditions (29), and after the saturation of LTP (28, 34).

NMDAR-STP, LTP and also LTD are most commonly studied in dorsal hippocampal slices (DHS) (23, 26, 35, 44-46), although they can be induced in many other brain areas e.g. (27, 28, 47-50). Interestingly, much smaller LTP and larger LTD have been reported in ventral hippocampal slices (VHS) when compared to dorsal (51-55), and most of the above literature on LTP suggests that NMDAR-STP is smaller in the ventral hippocampus than in the dorsal. The expression of NMDAR-independent forms of plasticity also differs significantly when compared across the dorsoventral hippocampal axis (56-59). The reasons for such intrahippocampal differences are not completely clear and a variety of explanations have been suggested.

Effects of NMDAR potentiators on NMDAR-STP and LTP in dorsal and ventral hippocampal slices

We have recently shown that NMDAR-STP, similar to LTP, is indeed smaller in VHS than in DHS (Fig 1C, (60)) and reported some interesting pharmacological observations with respect to the effects of NMDAR subunit-preferring potentiators on the induction of both NMDAR-STP and LTP (60). Notably, in experiments in DHS, in which two 4-pulse bursts (100 Hz) were delivered at theta frequency (2 × theta-burst stimulation, 2 × TBS, (43, 61)), the GluN2A/2B positive allosteric modulator (PAM, Table 1) UBP714 facilitated the induction of LTP but not NMDAR-STP, which did not change in its amplitude or decay time constant (Fig 1D). In these experiments submaximal levels of NMDAR-STP and LTP were observed.

However, in experiments in which either 5 × or 10 × TBS induced maximal levels of potentiation, the UBP714 effect on LTP was no longer observed (Fig 1D). These results demonstrate that subsaturated levels of LTP can be potentiated by enhancing NMDAR function. In VHS, where the level of LTP was lower than in DHS (Fig 1C), UBP714 facilitated the 10 × TBS-induced LTP and decreased the duration of NMDAR-STP, which would suggest sub-saturated LTP under the control conditions in the ventral slices (Fig 1E). Both the magnitude of NMDAR-STP and its duration could be increased in VHS by the GluN2C/D potentiator CIQ (Table 1), which had no effect on the induction of LTP (Fig 1F). The ability of UBP714 to speed up the decay of NMDAR-STP and the ability of CIQ to prolong the duration of NMDAR-STP are particularly noteworthy as it has been reported previously that the duration of STP varies significantly between different limbic areas, with two distinct types of STP – a fast and a slow, being readily discernible (27).

The differing effects of UBP714 and CIQ on NMDAR-STP and LTP in VHS also suggest that induction of these two forms of potentiation depends on discrete NMDAR subtypes, which is consistent with previous observations using different subunit-preferring NMDAR antagonists in DHS (62, 63). Indeed, a fast and a slow NMDAR-STP, which we termed STP1 and STP2 respectively, are sensitive to different subunit-preferring NMDAR antagonists in DHS (Fig 1G, (62)). The fast STP1 and LTP are particularly sensitive to GluN2A preferring antagonists NVP-AAM077 (NVP, Fig 1G and H) and AP5 (35, 62). The slow STP2 is particularly sensitive to the GluN2B antagonist Ro 25-6981 (Ro, Fig 1G and I) and the GluN2C/D antagonist UBP145 (Fig 1G and J). These antagonists have been characterised in detail (62, 64-69), both in recombinant receptor-systems and against native NMDARs in DHS (Table 1). The effects of these antagonists on NMDAR-STP or LTP in VHS have not been studied previously, and it is still unknown whether the levels of NMDAR-STP, which are induced in VHS, can be stored during pauses in the stimulation.

In the present study, we have characterised NMDAR-STP in VHS. Firstly, we have examined the effects of altering the number of TBS on the induction of NMDAR-STP and LTP, and the effects of a pause in stimulation on the maintenance of potentiation. Next, we have examined the sensitivity of ventral hippocampal NMDAR-STP and LTP to the same subtype-selective NMDAR antagonists (NVP, Ro and UBP145) as in our previous studies in the DHS (62, 63). Thirdly, we have explored how the sensitivity to these antagonists is influenced by the number of TBS delivered. We describe here that in VHS, NMDAR-STP and LTP differ in their sensitivity to NMDAR antagonists. We also show that the duration of

NMDAR-STP can be reliably modulated by the number of bursts delivered during TBS and that the fast and the slow types of NMDAR-STP (STP1 and STP2), induced by the specific paradigms, demonstrate differential sensitivity to some of the NMDAR antagonists. A graded induction of LTP, which increased in its sensitivity to NMDAR antagonists with stronger TBS, was also observed in VHS. These observations suggest that discrete NMDA receptors, activated by specific induction stimuli in a population of synapses, are responsible for the additive induction of specific types of potentiation.

Materials and methods

Slice preparation, electrophysiological recordings and chemicals

Experiments were performed after institutional approval, according to the UK Scientific Procedures Act, 1986 and European Union guidelines for animal care. Animals (male Wistar rats, 200-220 g, Charles River Lab UK) were sacrificed by cervical dislocation after isoflurane anaesthesia (Schedule 1). Transverse slices (400 μm) were cut from either the dorsal or the ventral pole of the hippocampus using a McIllwain tissue chopper, according to the procedures that were described previously in detail (23, 62). A total of 87 rats were used, producing 141 DHS and VHS recordings, reported in this paper.

Slices were pre-incubated at room temperature in artificial cerebrospinal fluid (ACSF) containing (in mM): NaCl (130), D-Glucose (10), $NaHCO_3$ (26), KCl (3.5), NaH_2PO_4 (1.2), $MgSO_4$ ($7H_2O$) (2) and $CaCl_2$ (2), for at least 2 h prior the start of the experiments. During the experiments, the slices were perfused at a rate of 2.5 ml/min and maintained submerged in ACSF (32 ºC). ACSF was saturated with 95% O_2 – 5% CO_2, in all conditions.

The Schaffer collaterals were stimulated using a platinum/iridium concentric bipolar electrode (CBAPB50, FHC USA) placed on the border between CA3 and CA2, in the stratum radiatum. Extracellular field excitatory postsynaptic potentials (fEPSPs) were recorded from the CA1 area of the stratum radiatum, using ACSF-filled borosilicate glass electrodes (1.5 – 3.5 MΩ). fEPSPs were amplified (MultiClamp 700A; Axon instruments), filtered at 3 kHz and digitised at 40 kHz (National Instruments, PCIe-6321). The stimulation current (A385; WPI) was set to three times the threshold current to elicit fEPSPs. WinLTP software (www.winltp.com) was used to control the timing of the experiments and to visualise and to record fEPSPs, which were stored on a PC (70).

Test stimulation was given once every 15 s (0.067 Hz), both before and after the induction of potentiation, and fEPSPs were recorded as the mean of 4 responses over a period of 1 min. Stability of baseline responses was monitored for at least 45 min prior to induction of potentiation. Potentiation was induced by TBS: 4 pulses delivered at 100 Hz, repeated either 10, 30 or 100 times at a 5 Hz frequency (10 × TBS, 30 × TBS or 100 × TBS). In all experiments, stimulation was interrupted for 3 min post-TBS to avoid PTP affecting the measurements of NMDAR-dependent plasticity (23). In experiments, in which NMDAR antagonists were used, compounds were bath applied for 30 min, after a 15 min recording of baseline potentials. Compounds were washed out following the TBS. Experiments were performed in an interleaved manner, randomising the application of different compounds and induction protocols.

NVP-AAM077 (NVP) and UBP145 were synthesised at the University of Bristol. Ro 25-6981 (Ro) and AP5 were purchased from Abcam (Cambridge, UK). All compounds were prepared as stock solutions, stored at -20°C and diluted to ACSF during the experiments. Detailed characterisation of these compounds has been published previously (62, 66, 67, 71).

Analysis of electrophysiological recordings and statistical analysis

The fEPSPs from individual experiments were quantified off-line by measuring the rate of rise (mV/ms) of their early initial slope (0.25 ms duration), after the termination of the fibre volley, corresponding to the steepest part of the fEPSP (confirmed by differentiation of the responses, Platin Calculator, Morten S. Jensen, Aarhus University, Denmark). The data were normalised to the baseline period, which was set at 100%, reflecting relative changes in the strength of synaptic transmission.

NMDAR-STP is sometimes (23, 62) but not always (27, 42, 62) induced as a uniformly decaying single exponential phenomenon. Due to the noise levels of individual experiments, and redundancy of mathematical models, double exponential functions cannot be used to reliably quantify the results, whilst single exponential functions discriminate reliably between fast- and slow-decaying NMDAR-STPs. Therefore, individual normalised experiments were curve fitted using a single-exponential decay function (Potentiation amplitude = LTP + STP $e^{-t/\tau}$), as described previously in (23), estimating the amplitudes of NMDAR-STP (%) and LTP (%), as well as the decay time constant of NMDAR-STP (τ, min). Statistical analyses of these parameters are reported in the Results, comparing the effects of different induction protocols on synaptic plasticity.

To estimate the inhibitory effects of the NMDAR antagonists on the induction of plasticity, NMDAR-STP was additionally quantified as the area under the decaying curve in individual experiments (NMDAR-STP$_{Area}$ = NMDAR-STP amplitude * τ). The % inhibition of NMDAR-STP$_{Area}$ could then be calculated, relative to the mean of the control without the application of antagonists, as described previously in DHS (62). Similarly, the % inhibition of LTP$_{Level}$ was calculated in individual experiments relative to the mean LTP amplitude without the application of antagonists. The inhibition of NMDAR-STP$_{Area}$ and LTP$_{Level}$ by the antagonists are reported and compared in the Results.

Time courses of potentiation are presented in the Results section as mean values of potentiation (%) ± standard error of the mean (SEM), plotted over time (h or min). For presentation, the individual data points are averaged over 2 min, with baseline levels subtracted. Results of all parameters and calculations are reported as mean values ± SEM. Unpaired two-tailed t-tests, and ANOVAs with a Tukey's or Dunnett's multiple comparison tests, were used for the between groups statistics (GraphPad Prism). Additionally, for more detailed presentation of the different potentiation components, some of the mean experimental datasets were fitted with either single or double exponential functions and these results are visualised in Figure 5. F-test was used to determine whether single or double exponential fit was most appropriate for the data (GraphPad Prism).

Results

Incremental induction of NMDAR-STP and LTP in ventral hippocampal slices

Ten 4-pulse 100 Hz bursts, delivered at a 5 Hz frequency (10 × TBS), are thought to be optimal in inducing maximal levels of potentiation in DHS (Fig 1D, (23, 43, 61, 72)). In the current DHS experiments, 10 × TBS induced NMDAR-STP (55.3 ± 4.5%) that declined with a τ value of 12.3 ± 1.5 min to a 47.9 ± 3.7% level of LTP (Fig 2A-D, black circles). The application of 10 × TBS in the VHS resulted in a smaller NMDAR-STP (39.2 ± 4.1%) that declined faster (τ = 6.6 ± 1.0 min) to a lower level of LTP (18.8 ± 2.3%) than in the DHS (Fig 2A-D, open and black circles, respectively). In both DHS and VHS, the decline of NMDAR-STP was use- but not time-dependent, in that a 30-min delay in stimulation suspended the decline of NMDAR-STP (Fig 2E, black circles vs white circles). This suggests that the process of NMDAR-STP storage might be similar in DHS and VHS. The differences in the magnitudes

of NMDAR-STP and LTP between DHS and VHS were not affected by introduction of a delay in stimulation (Fig 2F-H).

We next tested whether greater amounts of potentiation could be induced in VHS by increasing the number of theta bursts during the induction (Fig 2I-L). The amplitude of the 30 × TBS-induced NMDAR-STP (40.3 ± 4.3%, Fig 2I and J, white squares) was similar to the 10 x TBS-induced NMDAR-STP (39.2 ± 4.1%) but it declined with a much slower decay time constant (19.9 ± 1.7 min vs 6.6 ± 1.0 min, 30 and 10 × TBS respectively, Fig 2K). Significantly larger LTP was induced by 30 × TBS than by 10 × TBS (32.2 ± 2.8% vs 18.8 ± 2.3%, 30 and 10 × TBS respectively, Fig 2L). Such dependence of both τ and the magnitude of LTP on the number of stimuli during trains of stimulation has been previously reported in DHS (23). We have therefore tested whether a further increase in the number of theta bursts would result in a greater potentiation in VHS. However, the magnitudes of NMDAR-STP (42.7 ± 7.1% Fig 2J) and LTP (30.2 ± 4.4%, Fig 2L), and the decay time of NMDAR-STP (22.1 ± 3.5 min, Fig 2K), which were recorded in response to 100 × TBS (Fig 2I, grey triangles), were very similar to those in 30 × TBS (Fig 2I-L).

In summary, on the basis of the above experiments, we conclude that subsaturated levels of NMDAR-STP and LTP are induced in VHS by a 10 × TBS protocol. A dramatic slowing down of the decay of NMDAR-STP, and an increase in the levels of LTP, is observed with the stronger stimulation protocols. This suggests that incremental induction of NMDAR-STP and LTP leads to saturation of the potentiation processes in the VHS.

Sensitivity of ventral NMDAR-STP and LTP to GluN2 subunit-preferring NMDAR antagonists

Differential sensitivity of NMDAR-STP and LTP to GluN2 subunit-preferring NMDAR antagonists NVP, Ro and UBP145 (Table 1) has been observed in DHS (Fig 1G-J, (62)). Here, fast-decaying NMDAR-STP and LTP were particularly sensitive to low concentrations of NVP (10 – 100 nM), which show greatest selectivity to GluN2A subunits. In contrast, low concentrations of Ro (GluN2B-selective) and UBP145 (GluN2D-prefering) inhibited the induction of the slow-decaying NMDAR-STP and did not affect the induction of fast-decaying NMDAR-STP or LTP (Fig 1G-J).

NVP, Ro and UBP145 have not been tested on the induction of potentiation in VHS. Based on the previous results from DHS, and on the observation that 30 × TBS prolongs the decay of NMDAR-STP in VHS when compared to 10 × TBS (Fig 2I and L), we can predict a

greater sensitivity of the 10 × TBS-induced fast-decaying NMDAR-STP to NVP than when tested with 30 × TBS. Furthermore, we also predict a greater sensitivity of the 30 × TBS-induced slow-decaying NMDAR-STP to Ro and UBP145 than with 10 × TBS.

Much smaller NMDAR-STP (8.6 ± 2.2%, τ = 2.6 ± 1.1 min) and LTP (7.3 ± 1.8%) were induced by 10 × TBS (Fig 3A, pink circles) in experiments in which 0.1 μM NVP was applied for 30 min prior to tetanisation, when compared to the controls (Fig 3A, black circles, NMDAR-STP = 39.2 ± 4.1%, τ = 6.6 ± 1.0 min; LTP = 18.8 ± 2.3%). In contrast, a substantial slow-decaying NMDAR-STP (31.2 ± 8.7%, τ = 17.8 ± 4.1 min) was induced by 30 × TBS (Fig 3B, pink squares) in the presence of 0.1 μM NVP, whilst LTP (9.1 ± 8.0%) was greatly inhibited when compared to the experiments without the antagonist (Fig 3B, black squares, NMDAR-STP = 40.3 ± 4.3%, τ = 19.9 ± 1.7 min; LTP = 32.2 ± 2.8%). To assess these results quantitatively, we calculated % inhibition of NMDR-STP$_{Area}$ (Fig 3C) and % inhibition LTP$_{Level}$ (Fig 3D) and compared their inhibition between the 10 and the 30 × TBS groups. Thus, 0.1 μM NVP inhibited NMDAR-STP$_{Area}$ by 86.5 ± 7.3% in the 10 × TBS group compared to only 34.4 ± 16.9% in the 30 × TBS experiments (Fig 3C). The inhibition of LTP$_{Level}$ by NVP in the 10 × TBS group (61.2 ± 9.4%) was similar to that in 30 × TBS (71.6 ± 24.9%; Fig 3D). These results support the prediction that the sensitivity of NMDAR-STP to the GluN2A-preferring concentration of NVP decreases when the decay time constant of NMDAR-STP increases.

Application of 1 μM Ro (Fig 3E, light blue circles) in 10 × TBS experiments had no effect on the induction of NMDAR-STP (32.0 ± 5.0%, τ = 10.8 ± 2.9 min) or LTP (20.2 ± 2.7%), when compared to the control experiments without the application of the antagonist (Fig 3E, white circles, NMDAR-STP = 39.2 ± 4.1%, τ = 6.6 ± 1.0 min; LTP = 18.8 ± 2.3%). However, in the presence of a higher concentration of Ro (30 μM, dark blue circles), both NMDAR-STP (9.3 ± 1.9%, τ = 2.2 ± 0.9 min) and LTP (13.7 ± 2.7%) were smaller than in the control (Fig 3E, white circles). Effects of 1 μM Ro on the induction of NMDAR-STP became apparent in 30 × TBS experiments (Fig 3F, white vs light blue squares) in which NMDAR-STP (32.0 ± 5.3% vs 40.3 ± 4.3%) declined substantially faster (5.2 ± 1.1 min vs 19.9 ± 1.7 min) than in the controls, whilst LTP was largely unaffected (29.2 ± 3.7% vs 32.2 ± 2.8%, 1 μM Ro and controls respectively). Both NMDAR-STP (9.3 ± 1.9%, τ = 2.2 ± 0.9 min) and LTP (13.7 ± 2.7%) were inhibited by 30 μM Ro in 30 × TBS experiments (Fig 3F, dark blue vs white squares). Analyses of % inhibition of NMDAR-STP$_{Area}$ (Fig 3G) showed that 1 μM Ro inhibited NMDAR-STP more potently in experiments with 30 than with 10 × TBS. Similarly,

30 μM Ro inhibited 30 × TBS-induced LTP more potently than 10 × TBS induced LTP (Fig 3H). These results support the prediction that slow-decaying NMDAR-STP is more sensitive to the GluN2B antagonist Ro than fast-decaying NMDAR-STP. These experiments also show that the sensitivity of LTP to Ro increases, as the magnitude of LTP gets larger. However, although the sensitivity of both NMDAR-STP and LTP to the GluN2B antagonist increases as the number of the theta-bursts increases, a much higher concentration of Ro is needed to inhibit LTP than NMDAR-STP.

In contrast to NVP and Ro, application of 10 μM of UBP145 did not produce any differential effects on the induction of NMDAR-STP and LTP when compared between the 10 and the 30 × TBS experiments (Fig 3I and J, orange and white symbols). In both cases, the GluN2D antagonist inhibited most of the NMDAR-STP (Fig 3K) without affecting LTP (Fig 3L). Thus, NMDAR-STP (14.8 ± 4.3%) that was induced with 10 × TBS declined with a τ value of 1.3 ± 0.4 min to an LTP level of 19.2 ± 3.3% (Fig 3I, orange circles). A similarly small (10.9 ± 4.0%) and fast decaying (2.5 ± 1.5 min) NMDAR-STP was observed in the 30 × TBS experiments with UBP145 in which a large LTP (29.6 ± 8.6%) was still being observed (Fig 3J, orange squares). Such results suggest that both 10 and 30 × TBS-induced NMDAR-STP is particularly sensitive to UBP145, resulting in a near complete inhibition of NMDAR-STP without affecting LTP.

We were interested whether combined application of the different antagonists would permit inhibition of the residual phases of plasticity, which were observed in Fig 3. The residual LTP induced by the 10 × TBS paradigm was unaffected by combining 0.1 μM NVP, 10 μM UBP145 and 30 μM Ro (6.7 ± 1.2%, lilac circles, Fig 4A), indicating that the residual LTP phase (~ 7%) is not dependent on NMDAR activation (Fig 4B and C). We also tested 100 μM D-AP5 and found that it inhibited LTP to a similar extent (residual LTP = 8.1 ± 1.1%, n = 3, grey circles, Fig 4A and C).

In contrast to the 10 × TBS experiments, different combinations of the NMDAR antagonists produced a graded reduction in the slow-decaying NMDAR-STP in 30 × TBS experiments (Fig 4D), without further inhibition of the residual LTP (6 – 11%). Thus, the slowly decaying NMDAR-STP (31.2 ± 8.7%, τ = 17.8 ± 4.1 min), which was observed in the 0.1 μM NVP experiments (Fig 4D, pink squares), was sensitive to additional application of 10 μM UBP145 (NMDAR-STP = 18.4 ± 1.7%, τ = 3.0 ± 0.7 min, peach squares) and could be even further inhibited by a combination of the three antagonists together (NMDAR-STP = 6.5

± 2.9%, τ = 2.2 ± 1.2 min, lilac squares); suggesting that 30 × TBS-induced NMDAR-STP involves the activation of more than one NMDAR subtype.

Pharmacological segregation of the distinct potentiation components in the VHS, which were sensitive to NVP, Ro and UBP145, is shown in Fig 5 to collectively illustrate the relationships between intensity of TBS, slow- and fast-decaying STP, LTP, and the relative contribution of NMDAR subtypes. Notably, control NMDAR-STPs that were induced by 10 and 30 x TBS were best approximated by double exponential functions, whilst STPs that were recorded in the presence of either 0.1 μM NVP or 10 μM UBP145 were fitted best by single-exponentials, supporting the suggestion that NMDAR-dependent potentiation in VHS is a compound phenomenon that is composed of discrete phases of potentiation induced through graded activation of GluN2A, GluN2B and GluN2D containing NMDARs.

Discussion

NMDAR-STP and LTP in ventral and dorsal hippocampus

NMDAR-STP and LTP are two types of NMDAR-dependent synaptic plasticity that are co-induced in the hippocampus by extracellular high-frequency stimulation of the Schaffer collaterals. Consistent with previous publications, we report here that both NMDAR-STP and LTP are smaller in the VHS than in the DHS (51-55, 60).We also confirm that higher levels of LTP can be achieved in VHS by increasing the number of theta-bursts during the induction (73), although under our experimental conditions LTP in VHS saturated at a lower level than in DHS. The lower levels of potentiation induced in the ventral hippocampus when compared to the dorsal could potentially be due to different levels of NMDAR expression. Notably, some studies are finding a decrease in the receptor levels (74, 75), whilst others are reporting an increase in GluN1 and GluN2B expression in VHS (52). On the other hand, presynaptic factors may also be responsible for the induction of lower levels of NMDAR-STP and LTP in the ventral hippocampus than in the dorsal, in that the mechanisms of their induction depend on basal probability of neurotransmitter release (P_R). In support of such interpretation, PPF is reduced in ventral hippocampus when compared to dorsal (52, 54, 56-58, 76-79), suggesting a high P_R under baseline conditions in VHS. The amplitudes of both NMDAR-STP and LTP are directly related to baseline levels of PPF with large initial PPF leading to large NMDAR-STP

and/or LTP (23, 80), whilst the decay time constant of NMDAR-STP is independent on the basal PPF (23).

In contrast to LTP (51-55), NMDAR-STP has not been previously characterised in VHS in detail, and here we show that similar to the dorsal hippocampal NMDAR-STP (23, 24, 33, 62), the decay of NMDAR-STP in VHS requires presynaptic activity. Hence, when stimulation is stopped for 30 min after the induction, NMDAR-STP remains stored in VHS and its decay resumes only when the stimulation is re-commenced, indicating that the process of decay is not dependent on the overall magnitude of NMDAR-STP expression. The results also demonstrate that increasing the number of TBS in an induction protocol increases the duration of NMDAR-STP. This observation is in line with the previous study in DHS, showing that it is the number of stimuli in a tetanus that regulates the duration of NMDAR-STP (23). Thus, in VHS, 10 × TBS induces a fast-decaying NMDAR-STP and 30 × TBS induces a slower-decaying NMDAR-STP, supporting previous observations that two kinetically (27) and pharmacologically (62) different forms of NMDAR-STP can be induced within the hippocampus and in other limbic structures.

NMDAR-dependence of ventral NMDAR-STP and LTP in 10 x TBS experiments

Fast and slow decaying NMDAR-STP (termed STP1 and STP2, respectively), and LTP, rely on activation of different NMDAR subtypes in DHS and, by using the same NMDAR subunit-preferring antagonists as characterised previously (Fig 1G-J, Table 1, (62)), we have investigated here whether the induction of NMDAR-STP and LTP in VHS could also be dissected pharmacologically whilst using the 10 × TBS paradigm. 10 × TBS induces saturated NMDAR-STP and LTP in DHS (Fig 1C, also (43, 61)), and submaximal NMDAR-STP and LTP in VHS (Fig 2I). We expected fast decaying NMDAR-STP and LTP to be sensitive to NVP and slow decaying NMDAR-STP to be sensitive to Ro and UBP145.

In accord with our predictions, we found that the fast-decaying NMDAR-STP, and also LTP, induced by 10 × TBS were particularly sensitive to the GluN2A antagonist NVP (100 nM). NVP inhibited both types of potentiation close to their maximal extent, leaving a small NMDAR-independent LTP (Figs 3A, 4A and 5A). The fast NMDAR-STP was also inhibited by the GluN2D antagonist UBP145 (10 μM), which did not affect the induction of LTP (Figs 3I and 5A). Such inhibition of the fast component of NMDAR-STP by UBP145 was not observed in DHS, where UBP145 preferentially inhibited the slow component of NMDAR-STP (Fig 1G, (62)). Thus, inhibition of the fast component of NMDAR-STP by UBP145 may

be specific for the ventral hippocampus. In the VHS, the effects of NVP and UBP145 on the fast NMDAR-STP might be due to their inhibition of di-heteromeric GluN2D-containing receptors, or tri-heteromeric receptors containing both GluN2A and GluN2D subunits, in addition to the obligatory GluN1. The differential effect of NVP and UBP145 on LTP in VHS excludes involvement of GluN2Ds in LTP induction, just like in the DHS (62).

Notably, a GluN2B-selective concentration of Ro 25-6981 (1 μM) had neither an effect on NMDAR-STP nor on LTP, excluding the involvement of this subunit in the 10 × TBS experiments (Figs 3E and 5A). This appears in stark contrast to the published experiments in DHS, where 1 μM Ro decreases the decay time of NMDAR-STP, without affecting the induction of LTP (62). However, 10 × TBS in the DHS induces both fast and slow components of NMDAR-STP and 1 μM Ro inhibits only the slow component (Fig 1G). Such slow component of NMDAR-STP is less pronounced in 10 × TBS experiments in VHS (Figs 3E and 5A). Increasing the concentration of Ro to 30 μM inhibited the induction of both NMDAR-STP and LTP, producing very similar effects as 100 nM NVP on its own (Figs 3A, E and 4A). Ro does not inhibit GluN2D receptors, but can inhibit GluN2A at high concentrations (62, 67). We have previously noted that at concentrations above 10 μM, Ro starts inhibiting some GluN2A containing di-heteromeric receptors, with about 25% inhibition at 30 μM (62). It therefore seems possible that effects of high concentrations of Ro on NMDAR-STP and LTP are due to inhibition of NMDARs that contain GluN2A subunits, either in di- or in tri-heteromeric combinations. To the best of our knowledge, Ro has not been tested on tri-heteromeric receptors (please see (81, 82) for information on related compounds, such as ifenprodil and CP-101-606).

In summary, considering the cumulative results of the 10 × TBS experiments with the three antagonists, the inhibition of the fast NMDAR-STP in 10 × TBS experiments might be mediated by inhibition of GluN2A/2D-containing NMDARs (sensitive to NVP, UBP145 and high concentrations of Ro) whilst the inhibition of LTP could be mediated by inhibition of GluN2A- or GluN2A/2B-containing receptors (sensitive to NVP and high concentrations of Ro).

NMDAR-dependence of ventral NMDAR-STP and LTP in 30 × TBS experiments

The slow, 30 × TBS-induced NMDAR-STP appeared to be pharmacologically distinct from the fast 10 × TBS-induced NMDAR-STP. Thus, 100 nM NVP did not inhibit NMDAR-STP completely but preserved a large slowly-decaying component of NMDAR-STP (Figs 3B

and 5B). LTP, however, was inhibited by NVP to roughly the same extent as in the 10 × TBS experiments (Figs 3D and 5B), which means the NMDAR subunit that mediates induction of the slow NMDAR-STP does not contribute to the induction of LTP.

UBP145 inhibited the slow, 30 × TBS-induced NMDAR-STP completely, suggesting that GluN2D receptors are involved in its induction in VHS (Figs 3J-K and 5B). These results show that while UBP145 inhibits both the fast and the slow decaying NMDAR-STP without affecting LTP (Figs 3L and 5B), NVP inhibits only the fast component of NMDAR-STP, and also LTP. Such results suggest involvement of an additional subunit in the 30 × TBS induction of NMDAR-STP when compared to 10 × TBS, which could be GluN2B, as it has the lowest affinity to NVP when compared to the other subunits. In support of that conclusion, 1 μM Ro decreased the decay time constant of NMDAR-STP in 30 × TBS experiments and did not affect the induction of LTP (Figs 3F-H and 5B); this effect being similar to the effect of 1 μM Ro on NMDAR-STP in DHS (Fig 1G), as discussed above.

Increasing the concentration of Ro to 30 μM in the 30 × TBS experiments inhibited both NMDAR-STP and LTP, similar to the results in 10 × TBS experiments in VHS, and also in the DHS, as published previously (62). The amount of LTP, that was inhibited by 30 μM Ro was significantly larger in the 30 × TBS than 10 × TBS experiments. However, this increased sensitivity of LTP to 30 μM Ro is unlikely to indicate involvement of di-heteromeric GluN2B-containing receptors in the induction of LTP, as it remained insensitive to 1 μM Ro (Fig 5B). We therefore currently believe that a pharmacologically homogeneous population of NMDARs, composed of either di-heteromeric GluN2A-containing receptors or of tri-heteromeric receptors that contain both GluN2A and GluN2B subunits, mediates induction of LTP in both 10 × TBS and 30 × TBS experiments. On the other hand, considering the effects of Ro we have to note that this antagonist has a complex allosteric mechanism of action: it does not produce 100% inhibition of di-heteromeric GluN2B-containing NMDARs (62) and it can even facilitate GluN2B responses at low agonist concentrations (62, 67). Therefore, the effects of Ro on synaptic plasticity may be difficult to interpret, involving changes in efficacy and contribution of spare receptors.

Segregation of the fast and slow NMDAR-STP, and LTP in VHS

Although, as discussed above, we cannot be completely certain about the exact composition of the LTP-inducing NMDARs (i.e. GluN2As vs GluN2A/Bs) in VHS we can still be confident that these receptors are pharmacologically different from the receptors that

mediate the induction of NMDAR-STP. The fast NMDAR-STP in VHS is likely induced by NMDARs that contain GluN2A and GluN2D subunits, whilst the slow NMDAR-STP is induced through NMDARs containing GluN2Bs and GluN2Ds. Importantly, the two types of NMDAR-STP in VHS differ not only from each other in terms of NMDAR subunits involved, but also from LTP, which does not require involvement of GluN2Ds (Fig 5). Such complete segregation of the fast STP1, the slow STP2 and LTP was not that obvious in DHS (Fig 1G-J, (62)) where STP1 lacked sensitivity to inhibition of GluN2Ds and was more akin to LTP in terms of sensitivity to GluN2As. Sensitivity of the slow STP2 to inhibition of GluN2B/2D subunits is shared between the dorsal and the ventral hippocampus. The effects of NMDAR inhibitors in the VHS are in line with the previously published results using GluN2 subunit potentiators (Fig 1E and F, (60)). Here, the GluN2A/2B-preferring PAM UBP714 potentiated induction of LTP and decreased the decay time constant of NMDAR-STP, while the GluN2C/D-preferring PAM CIQ increased the amplitude of NMDAR-STP and slowed its decay, without affecting induction of LTP. Activation of the slow NMDAR-STP requires prolonged tetanisation in the VHS, which might suggest that higher concentrations of glutamate (or glutamate spillover) are required to activate NMDARs that are responsible for its induction. Such NMDARs might be located either extra- or peri-synaptically, on either pre- or postsynaptic terminals, and future investigations will have to be conducted in order to determine sub-cellular locations of these receptor complexes.

Final remarks - wider pharmacological implications for the study of synaptic plasticity

The results presented in this publication show that the sensitivity of both NMDAR-STP and LTP to NMDAR antagonists (NVP and Ro) changes dependent on the duration of TBS and the magnitude of synaptic plasticity induced. Such differential sensitivity, which corresponds to the level of agonist-evoked biological effect, is likely to complicate comparison between different studies that use single concentrations of antagonists to investigate synaptic plasticity in preparations without clearly defined maximal effects. Many previous studies used NVP and Ro to infer conclusions about NMDAR subunit involvement (or lack of involvement) in regulating the induction of LTP and LTD, and we have discussed the disparity of the results in earlier publications (5, 60, 62). On this occasion we can only stress that our current observations extend beyond the use of NMDAR antagonists, and that without comparing “like with like” we shall be probably discussing the basic principles of pharmacology during the 60th celebration of LTP.

Acknowledgements

We would like to acknowledge The Royal Society (RSG\R1\180384; AV) and the Blizard Institute, QMUL for supporting this study. We further acknowledge support by CIHR (Canadian Institutes of Health Research) Foundation Grant #154276 to GLC and a Krembil Foundation grant to GLC and JG. GLC is the holder of the Krembil Family Chair in Alzheimer's Research.

Supplementary material
None included.

Authors' contributions
AV and RI designed the study. RI performed all experiments in the VHS and some in DHS. RV performed some of the experiments in the DHS. RI and RV analysed the data and, together with AV, wrote the first draft of the manuscript. DEJ supervised pharmacology. JG, ATM-T, GLC and AV supervised the electrophysiological experiments. All authors have read, commented on and approved the final version.

Funding
Supported by The Royal Society (RSG\R1\180384) and the Blizard Institute. We further acknowledge support by CIHR (Canadian Institutes of Health Research) Foundation Grant #154276 to GLC and a Krembil Foundation grant to GLC and JG. GLC is the holder of the Krembil Family Chair in Alzheimer's Research.

Availability of data and materials
All data and their analyses are included in this paper any additional information is available from the corresponding author on reasonable request.

Ethics
Experiments were performed after institutional approval and according to national and EU guidelines for animal care using Schedule 1 procedures for tissue preparation (the UK Scientific Procedures Act, 1986).

Consent for publication
Not applicable.

Competing interests
G.L.C. and D.E.J. are on the Scientific Advisory Board of Hello Bio.

Figure captions

Fig 1. NMDAR-dependence of NMDAR-STP and LTP in the hippocampus (previously published (5, 60, 62)).

A. Mean time course of potentiation (black circles ± SEM) induced by 10 × TBS in dorsal hippocampal slices (DHS). NMDAR-dependent short-term potentiation (STP) declined to a steady level of LTP in about 1 hour (data from (5)). Application of AP5 (red line) inhibited the induction of both NMDAR-STP and LTP (grey circles; data from (62)).

B. Decay of NMDAR-STP is not time-dependent and its levels can be maintained during periods without stimulation (yellow – 15 min, green – 30 min, red – 45 min; data from 5). Grey circles show an experiment in which induction of NMDAR-STP and LTP were inhibited by AP5 (data from (62)).

C. 10 × TBS induces smaller NMDAR-STP and LTP in ventral hippocampal slices (VHS, white circles) when compared to both 5 × and 10 × TBS in DHS (data from (60)).

D. GluN2A/2B potentiator UBP714 (brown symbols) facilitates induction of LTP in 2 × TBS experiments but not in 5 or 10 × TBS experiments in DHS (data from (60)).

E. UBP714 (brown circles) shortens the decay of NMDAR-STP and facilitates induction of LTP in 10 × TBS experiments in VHS (data from (60)).

F. GluN2C/D potentiator CIQ (brown circles) facilitates induction of larger NMDAR-STP and prolongs its decay in VHS. CIQ does not enhance LTP (data from (60)).

G. GluN2A-prefering antagonist NVP (pink circles) blocks LTP and inhibits fast STP1 whilst preserving STP2. GluN2B antagonist Ro (light blue circles) and GluN2C/2D-prefering antagonist UBP145 (orange circles) inhibit slow STP2 and do not affect STP1or LTP. Control is shown in black (all data from (62)).

H, **I** and **J**. Full concentration response curves for inhibition of STP1, STP2 and LTP by NVP, Ro and UBP145 in DHS. The rank order potency of the antagonists for the different GluN2 subunits was determined in HEK293 cells (all data replotted from (62)).

Fig 2. The magnitude of hippocampal NMDAR-STP and LTP is dependent on slice preparation and the number of theta bursts delivered.

A. Pooled data showing the time courses of potentiation of fEPSPs (mean ± SEM) for DHS (black circles) and VHS (white circles). The coloured letters depict the timing of the fEPSPs, shown to the right.

B. The amplitude of NMDAR-STP was significantly greater in DHS compared to VHS (55.3 ± 4.5% vs 39.2 ± 4.1%, $p = 0.016$).

C. The decay time constant of NMDAR-STP was greater in DHS (12.3 ± 1.5 min) than in VHS (6.6 ± 1.0 min; $p = 0.0025$).

D. The LTP was larger in the DHS compared to the VHS (47.9 ± 3.7% vs 18.8 ± 2.3%, $p < 0.0001$).

E. NMDAR-STP is stored when test stimulation is paused for 30 min in both DHS (black circles) and VHS (white circles).

F. The amplitude of stored NMDAR-STP is greater in DHS compared to VHS (53.6 ± 4.6% vs 27.1 ± 3.9%, $p = 0.00037$).

G. NMDAR-STP decayed at a slower rate in DHS (11.9 ± 1.7 min) than in VHS (6.5 ± 1.7 min; $p = 0.039$).

H. LTP was greater in DHS compared to VHS (47.4 ± 5.5% vs 20.7 ± 2.4%; $p = 0.00064$).

I. Time course of NMDAR-STP and LTP induced by 10 × TBS (white circles; results from panel A are reproduced in panel I), 30 × TBS (white squares) and 100 × TBS (grey triangles) in VHS.

J. The amplitude of NMDAR-STP was similar for all three inductions paradigms; 39.2 ± 4.1% (10 × TBS), 40.3 ± 4.3% (30 × TBS) and 42.7 ± 7.1% (100 × TBS; $p = 0.94$, ANOVA).

K. The rate of NMDAR-STP decay was significantly faster in the 10 × TBS group (6.6 ± 1.0 min) compared to the 30 × TBS experiments (19.9 ± 1.7 min; $p < 0.0001$, Tukey's multiple comparisons test) and the 100 × TBS group (22.1 ± 3.5 min; $p = 0.0003$, Tukey's multiple comparisons test).

L. LTP was greater in the 30 × TBS (32.2 ± 2.8%) group compared to 10 × TBS (18.8 ± 2.3%, $p = 0.0016$, Tukey's multiple comparisons test), whilst 100 × TBS did not induce any more LTP (30.2 ± 4.4%, $p = 0.95$, Tukey's multiple comparisons test).

Fig 3. Discrete sensitivity of NMDAR-STP and LTP to different NMDAR antagonists in VHS.

A. Time course of potentiation induced by 10 × TBS in the presence of 0.1 μM GluN2A-preferring antagonist NVP (pink circles) and the control experiments (white circles).

B. Time course of NMDAR-STP and LTP induced by 30 × TBS in the presence of 0.1 μM NVP (pink squares) and in controls (white squares).

C. NMDAR-STP_{Area} (STP_{Area}) induced by 10 × TBS was inhibited to a greater extent by 0.1 μM NVP compared to the 30 × TBS group with 86.5 ± 7.3% and 34.4 ± 16.9% inhibition, respectively ($p = 0.0063$).

D. NVP inhibited LTP_{Level} induced by 10 × TBS (61.2 ± 9.4%) and 30 × TBS (71.6 ± 24.9%) to a similar extent ($p = 0.64$).

E. Potentiation induced by 10 × TBS in the presence of 1 μM (light blue circles) and 30 μM (dark blue circles) Ro.

F. NMDAR-STP and LTP induced by 30 × TBS with the application of 1 μM (light blue squares) and 30 μM (dark blue squares) GluN2B-preferring antagonist, Ro.

G. NMDAR-STP_{Area} induced by 10 × TBS was not sensitive to 1 μM Ro (-1.9 ± 13.6% inhibition), whereas, NMDAR-STP_{Area} induced by 30 × TBS was highly sensitive to 1 μM Ro (78.7 ± 5.2% inhibition, $p = 0.00064$). Ro at 30 μM inhibited NMDAR-STP_{Area} induced by both 10 and 30 × TBS similarly (93.5 ± 2.4% and 89.3 ± 3.1%, $p = 0.31$).

H. 1 μM Ro did not significantly inhibit LTP_{Level} and its effects were similar when compared between 10 or 30 x TBS (-7.4 ± 14.2% and 9.1 ± 11.6%, $p = 0.40$). LTP_{Level} induced by 30 x TBS was more sensitive to the presence of 30 μM Ro (66.3 ± 7.5%) than 10 x TBS induced LTP (27.1 ± 14.5%, $p = 0.043$).

I. NMDAR-STP and LTP induced by 10 × TBS in the presence of 10 μM GluN2D-preferring antagonist, UBP145 (orange circles).

J. Potentiation induced by 30 × TBS in the presence of 10 μM UBP145 (orange squares).

K. 10 μM UBP145 inhibited 10 and 30 × TBS-induced NMDAR-STP_{Area} to a similar extent (90.7 ± 4.5% and 93.7 ± 4.9% inhibition, respectively, $p = 0.66$).

L. UBP145 did not inhibit the induction of LTP_{Level} and its effects were similar when compared between 10 × TBS (-2.5 ± 17.7% inhibition) and 30 × TBS groups (8.0 ± 26.8% inhibition, $p = 0.75$).

Fig 4. Incremental sensitivity of 30 × TBS-induced NMDAR-STP to NMDAR antagonists.

A. Time courses of potentiation induced by 10 × TBS in control experiments (white circles), in the presence of GluN2A-preferring antagonist NVP (pink circles), with NVP and GluN2D-preferring antagonist UBP145 (peach circles), and with NVP, UBP145 and GluN2B-preferring antagonist Ro (lilac circles). Grey circles show experiments with AP5.

B. NMDAR-STP$_{Area}$ was inhibited to a similar extent when compared between the four conditions ($p = 0.75$, ANOVA): 86.5 ± 7.3% for NVP alone, 95.0 ± 2.1% with the addition of UBP145, or 95.3 ± 2.6% with the addition of both UBP145 and Ro, and 87.2 ± 8.8% for AP5.

C. LTP$_{Level}$ was inhibited to a similar extent $p = 0.95$ (ANOVA), for the four in-between group comparisons: 61.2 ± 9.4% (NVP), 65.5 ± 3.9% (NVP and UBP145), 64.1 ± 6.5% (NVP, UBP145 and Ro) and 56.9 ± 5.9% (AP5).

D. Time courses of potentiation induced by 30 × TBS in the control experiments white squares), in the presence of NVP (pink squares), with NVP and UBP145 (peach squares), and with NVP, UBP145 and Ro (lilac squares).

E. NMDAR-STP$_{Area}$ was inhibited to a greater extent by a combination of either NVP and UBP145 (93.2 ± 1.3% inhibition, $p = 0.0056$, Dunnett's multiple comparisons test) or NVP, UBP145 and Ro together (96.5 ± 2.8%, $p = 0.0026$, Dunnett's multiple comparisons test) compared to only NVP (34.4 ± 16.9% inhibition, $p = 0.0023$, ANOVA).

F. There was no difference ($p = 0.79$, ANOVA) in the amount of inhibition of LTP$_{Level}$ by NVP (71.6 ± 23.9%) compared to NVP plus UBP145 (64.6 ± 5.4%) or NVP, UBP145 and Ro all combined (82.0 ± 12.2%).

Fig 5. NMDAR-dependent potentiation components in the VHS

A. Mean 10 x TBS induced control potentiation (Ctrl, white circles, n = 20) was fitted better with a double-exponential function (thick black dashed line, 90 min fit duration) than with single exponential function (F test, $F(2,915) = 5.739$; $p = 0.0033$), producing estimates of fast- and slow-decaying NMDAR-STP (STP1 and STP2, respectively) and LTP. 1 μM Ro did not inhibit NMDAR-STP or LTP induced by 10 x TBS and these results were also fitted with a double-exponential function (blue dashed line, mean data Fig 3E). On the contrary, mean time courses of potentiation that were induced in the presence of 10 μM UBP145 (NMDAR-STP = 14.1%, $\tau = 1.1$ min, LTP = 19%, white dashed line, mean data Fig 3I) or 0.1 μM NVP (NMDAR-STP = 4.6%, $\tau = 12.5$ min, LTP = 7%, yellow dashed line, mean data Fig 3A) were better fit by single-exponential curves than by double, and both antagonists inhibited NMDAR-dependent potentiation. Amounts of potentiation that were inhibited by the antagonists are visualised with solid colours (areas above the fitted curves). UBP145 partially inhibited NMDAR-STP but not LTP (solid orange, area above white dashed line). In addition to the orange area inhibited by UBP145, 0.1 μM NVP inhibited a large amount of NMDAR-STP and fully inhibited NMDAR-dependent LTP (solid pink, area above yellow dashed line). The small, residual, NVP-insensitive component of STP (solid lilac) was inhibited by a mixture (Mix) of UBP145 (10 μM), NVP (0.1 μM) and Ro (30 μM). Black area, derived by fitting single exponential function to the Mix of the antagonists (mean data Fig 4A), visualises NMDAR-independent component of LTP.

B. 30 x TBS experiments are presented in the same way as 10 x TBS experiments above. Once again, both the controls (white squares, n = 16, thick black dashed line, $F(2,731) = 7.938$; $p = 0.0004$) and the experiments using 1 μM Ro (blue dashed line, $F(2,225) = 5.015$; $p = 0.0074$, mean data Fig. 3F) were better fit with double exponential functions whilst 10 μM UBP145 (NMDAR-STP = 9.2%, $\tau = 3.3$ min, LTP = 28%, white dashed line, mean data Fig 3J) and 0.1 μM NVP (NMDAR-STP = 30.3%, $\tau = 12.8$ min, LTP = 11%, yellow dashed line, mean data Fig 3B) were better approximated by single exponential functions. The orange component of NMDAR-STP above the blue 1 μM Ro line can be inhibited by both Ro and UBP145. The green solid inclusion area indicates the small amount of NMDAR-STP that is inhibited by UBP145 and preserved by NVP. The large, residual NVP-insensitive component of STP (solid lilac) is inhibited by the Mix of UBP145 (10 μM), NVP (0.1 μM) and Ro (30 μM). Black area, derived by fitting single exponential function to the Mix of the antagonists (mean data Fig 4B), visualises NMDAR-independent component of LTP.

References

1. Bliss TV, Collingridge GL. A synaptic model of memory: long-term potentiation in the hippocampus. Nature. 1993;361(6407):31-9.
2. Abraham WC. How long will long-term potentiation last? Philos Trans R Soc Lond B Biol Sci. 2003;358(1432):735-44.
3. Raymond CR. LTP forms 1, 2 and 3: different mechanisms for the "long" in long-term potentiation. Trends Neurosci. 2007;30(4):167-75.
4. Zucker RS, Regehr WG. Short-term synaptic plasticity. Annu Rev Physiol. 2002;64:355-405.
5. Volianskis A, France G, Jensen MS, Bortolotto ZA, Jane DE, Collingridge GL. Long-term potentiation and the role of N-methyl-D-aspartate receptors. Brain Res. 2015;1621:5-16.
6. Park P, Volianskis A, Sanderson TM, Bortolotto ZA, Jane DE, Zhuo M, et al. NMDA receptor-dependent long-term potentiation comprises a family of temporally overlapping forms of synaptic plasticity that are induced by different patterns of stimulation. Philos Trans R Soc Lond B Biol Sci. 2014;369(1633):20130131.
7. Alkadhi KA. NMDA receptor-independent LTP in mammalian nervous system. Prog Neurobiol. 2021;200:101986.
8. Sacktor TC, Fenton AA. What does LTP tell us about the roles of CaMKII and PKMzeta in memory? Mol Brain. 2018;11(1):77.
9. Bliss TV, Collingridge GL. Expression of NMDA receptor-dependent LTP in the hippocampus: bridging the divide. Mol Brain. 2013;6:5.
10. Martin SJ, Grimwood PD, Morris RG. Synaptic plasticity and memory: an evaluation of the hypothesis. Annu Rev Neurosci. 2000;23:649-711.
11. Bliss TV, Lomo T. Long-lasting potentiation of synaptic transmission in the dentate area of the anaesthetized rabbit following stimulation of the perforant path. J Physiol. 1973;232(2):331-56.
12. Bliss TV, Gardner-Medwin AR. Long-lasting potentiation of synaptic transmission in the dentate area of the unanaestetized rabbit following stimulation of the perforant path. J Physiol. 1973;232(2):357-74.
13. Stevens CF. A million dollar question: does LTP = memory? Neuron. 1998;20(1):1-2.
14. Zucker RS. Short-term synaptic plasticity. Annu Rev Neurosci. 1989;12:13-31.
15. Kamiya H, Zucker RS. Residual Ca2+ and short-term synaptic plasticity. Nature. 1994;371(6498):603-6.
16. Jensen K, Jensen MS, Lambert JD. Post-tetanic potentiation of GABAergic IPSCs in cultured rat hippocampal neurones. J Physiol. 1999;519 Pt 1(Pt 1):71-84.
17. Lansner A, Fiebig F, Herman P. Fast Hebbian plasticity and working memory. Curr Opin Neurobiol. 2023;83:102809.
18. Durstewitz D, Seamans JK, Sejnowski TJ. Neurocomputational models of working memory. Nat Neurosci. 2000;3 Suppl:1184-91.
19. Goddard GV. Progress on the Physiological Bases of Memory. Brain and Behaviour Proceedings of the 28th International Congress of Physiological Sciences, Budapest, 1980: Elsevier; 1981. p. 525-32.
20. Goddard GV. Component Properties of the Memory Machine: Hebb Revisited. In: Jusczyk PW, Klein RM, editors. The Nature of Thought: Essays in Honor of Do Hebb. eBook (first edition 1981) ed. New Jersey.: Psychology Press.; 2014. p. 231-47.
21. Hebb DO. Distinctive features of learning in the higher animal. In: Delafresnaye JF, editor. Brain mechanisms and learning, a Symposium. Oxford: Blackwell; 1961. p. 37–46.
22. Kandel ER, Spencer WA. Cellular neurophysiological approaches in the study of learning. Physiol Rev. 1968;48(1):65-134.

23. Volianskis A, Jensen MS. Transient and sustained types of long-term potentiation in the CA1 area of the rat hippocampus. J Physiol. 2003;550(Pt 2):459-92.
24. Volianskis A, Collingridge GL, Jensen MS. The roles of STP and LTP in synaptic encoding. PeerJ. 2013;1:e3.
25. Ingram R, Kang H, Lightman S, Jane DE, Bortolotto ZA, Collingridge GL, et al. Some distorted thoughts about ketamine as a psychedelic and a novel hypothesis based on NMDA receptor-mediated synaptic plasticity. Neuropharmacology. 2018;142:30-40.
26. Collingridge GL, Kehl SJ, McLennan H. Excitatory amino acids in synaptic transmission in the Schaffer collateral-commissural pathway of the rat hippocampus. J Physiol. 1983;334:33-46.
27. Racine RJ, Milgram NW. Short-term potentiation phenomena in the rat limbic forebrain. Brain Res. 1983;260(2):201-16.
28. Racine RJ, Milgram NW, Hafner S. Long-term potentiation phenomena in the rat limbic forebrain. Brain Res. 1983;260(2):217-31.
29. McNaughton BL. Long-term synaptic enhancement and short-term potentiation in rat fascia dentata act through different mechanisms. J Physiol. 1982;324:249-62.
30. Stevens CF, Tonegawa S, Wang Y. The role of calcium-calmodulin kinase II in three forms of synaptic plasticity. Curr Biol. 1994;4(8):687-93.
31. Hinds HL, Tonegawa S, Malinow R. CA1 long-term potentiation is diminished but present in hippocampal slices from alpha-CaMKII mutant mice. Learn Mem. 1998;5(4-5):344-54.
32. Korshoej AR, Lambert JD. Post-tetanic potentiation of GABAergic IPSCs in cultured hippocampal neurons is exclusively time-dependent. Brain Res. 2007;1138:39-47.
33. Pradier B, Lanning K, Taljan KT, Feuille CJ, Nagy MA, Kauer JA. Persistent but Labile Synaptic Plasticity at Excitatory Synapses. J Neurosci. 2018;38(25):5750-8.
34. Schulz PE, Fitzgibbons JC. Differing mechanisms of expression for short- and long-term potentiation. J Neurophysiol. 1997;78(1):321-34.
35. Malenka RC. Postsynaptic factors control the duration of synaptic enhancement in area CA1 of the hippocampus. Neuron. 1991;6(1):53-60.
36. Debanne D, Gahwiler BH, Thompson SM. Heterogeneity of synaptic plasticity at unitary CA3-CA1 and CA3-CA3 connections in rat hippocampal slice cultures. J Neurosci. 1999;19(24):10664-71.
37. Selig DK, Nicoll RA, Malenka RC. Hippocampal long-term potentiation preserves the fidelity of postsynaptic responses to presynaptic bursts. J Neurosci. 1999;19(4):1236-46.
38. Pananceau M, Chen H, Gustafsson B. Short-term facilitation evoked during brief afferent tetani is not altered by long-term potentiation in the guinea-pig hippocampal CA1 region. J Physiol. 1998;508 (Pt 2)(Pt 2):503-14.
39. Yasui T, Fujisawa S, Tsukamoto M, Matsuki N, Ikegaya Y. Dynamic synapses as archives of synaptic history: state-dependent redistribution of synaptic efficacy in the rat hippocampal CA1. J Physiol. 2005;566(Pt 1):143-60.
40. Markram H, Tsodyks M. Redistribution of synaptic efficacy between neocortical pyramidal neurons. Nature. 1996;382(6594):807-10.
41. Markram H, Tsodyks M. Redistribution of synaptic efficacy: a mechanism to generate infinite synaptic input diversity from a homogeneous population of neurons without changing absolute synaptic efficacies. J Physiol Paris. 1996;90(3-4):229-32.
42. Erickson MA, Maramara LA, Lisman J. A single brief burst induces GluR1-dependent associative short-term potentiation: a potential mechanism for short-term memory. J Cogn Neurosci. 2010;22(11):2530-40.
43. Larson J, Wong D, Lynch G. Patterned stimulation at the theta frequency is optimal for the induction of hippocampal long-term potentiation. Brain Res. 1986;368(2):347-50.

44. Andersen P, Sundberg SH, Sveen O, Wigstrom H. Specific long-lasting potentiation of synaptic transmission in hippocampal slices. Nature. 1977;266(5604):736-7.
45. Lynch GS, Dunwiddie T, Gribkoff V. Heterosynaptic depression: a postsynaptic correlate of long-term potentiation. Nature. 1977;266(5604):737-9.
46. Dudek SM, Bear MF. Homosynaptic long-term depression in area CA1 of hippocampus and effects of N-methyl-D-aspartate receptor blockade. Proc Natl Acad Sci U S A. 1992;89(10):4363-7.
47. Collingridge GL, Peineau S, Howland JG, Wang YT. Long-term depression in the CNS. Nat Rev Neurosci. 2010;11(7):459-73.
48. Yashiro K, Philpot BD. Regulation of NMDA receptor subunit expression and its implications for LTD, LTP, and metaplasticity. Neuropharmacology. 2008;55(7):1081-94.
49. Harsanyi K, Friedlander MJ. Transient synaptic potentiation in the visual cortex. II. Developmental regulation. J Neurophysiol. 1997;77(3):1284-93.
50. Harsanyi K, Friedlander MJ. Transient synaptic potentiation in the visual cortex. I. Cellular mechanisms. J Neurophysiol. 1997;77(3):1269-83.
51. Colgin LL, Kubota D, Jia Y, Rex CS, Lynch G. Long-term potentiation is impaired in rat hippocampal slices that produce spontaneous sharp waves. J Physiol. 2004;558(Pt 3):953-61.
52. Dubovyk V, Manahan-Vaughan D. Less means more: The magnitude of synaptic plasticity along the hippocampal dorso-ventral axis is inversely related to the expression levels of plasticity-related neurotransmitter receptors. Hippocampus. 2018;28(2):136-50.
53. Maggio N, Segal M. Unique regulation of long term potentiation in the rat ventral hippocampus. Hippocampus. 2007;17(1):10-25.
54. Milior G, Di Castro MA, Sciarria LP, Garofalo S, Branchi I, Ragozzino D, et al. Electrophysiological Properties of CA1 Pyramidal Neurons along the Longitudinal Axis of the Mouse Hippocampus. Sci Rep. 2016;6:38242.
55. Papatheodoropoulos C, Kostopoulos G. Decreased ability of rat temporal hippocampal CA1 region to produce long-term potentiation. Neurosci Lett. 2000;279(3):177-80.
56. Papatheodoropoulos C, Kostopoulos G. Dorsal-ventral differentiation of short-term synaptic plasticity in rat CA1 hippocampal region. Neurosci Lett. 2000;286(1):57-60.
57. Tidball P, Burn HV, Teh KL, Volianskis A, Collingridge GL, Fitzjohn SM. Differential ability of the dorsal and ventral rat hippocampus to exhibit group I metabotropic glutamate receptor-dependent synaptic and intrinsic plasticity. Brain Neurosci Adv. 2017;1(1).
58. Samara MA, Oikonomou GD, Trompoukis G, Madarou G, Adamopoulou M, Papatheodoropoulos C. Septotemporal variation in modulation of synaptic transmission, paired-pulse ratio and frequency facilitation/depression by adenosine and GABA(B) receptors in the rat hippocampus. Brain Neurosci Adv. 2022;6:23982128221106315.
59. Moschovos C, Papatheodoropoulos C. The L-type voltage-dependent calcium channel long-term potentiation is higher in the dorsal compared with the ventral associational/commissural CA3 hippocampal synapses. Neurosci Res. 2016;106:62-5.
60. France G, Volianskis R, Ingram R, Bannister N, Rotharmel R, Irvine MW, et al. Differential regulation of STP, LTP and LTD by structurally diverse NMDA receptor subunit-specific positive allosteric modulators. Neuropharmacology. 2022;202:108840.
61. Larson J, Lynch G. Induction of synaptic potentiation in hippocampus by patterned stimulation involves two events. Science. 1986;232(4753):985-8.
62. Volianskis A, Bannister N, Collett VJ, Irvine MW, Monaghan DT, Fitzjohn SM, et al. Different NMDA receptor subtypes mediate induction of long-term potentiation and two

forms of short-term potentiation at CA1 synapses in rat hippocampus in vitro. J Physiol. 2013;591(4):955-72.
63. France G, Fernandez-Fernandez D, Burnell ES, Irvine MW, Monaghan DT, Jane DE, et al. Multiple roles of GluN2B-containing NMDA receptors in synaptic plasticity in juvenile hippocampus. Neuropharmacology. 2017;112(Pt A):76-83.
64. Buller AL, Monaghan DT. Pharmacological heterogeneity of NMDA receptors: characterization of NR1a/NR2D heteromers expressed in Xenopus oocytes. Eur J Pharmacol. 1997;320(1):87-94.
65. Mullasseril P, Hansen KB, Vance KM, Ogden KK, Yuan H, Kurtkaya NL, et al. A subunit-selective potentiator of NR2C- and NR2D-containing NMDA receptors. Nat Commun. 2010;1:90.
66. Feng B, Tse HW, Skifter DA, Morley R, Jane DE, Monaghan DT. Structure-activity analysis of a novel NR2C/NR2D-preferring NMDA receptor antagonist: 1-(phenanthrene-2-carbonyl) piperazine-2,3-dicarboxylic acid. Br J Pharmacol. 2004;141(3):508-16.
67. Fischer G, Mutel V, Trube G, Malherbe P, Kew JN, Mohacsi E, et al. Ro 25-6981, a highly potent and selective blocker of N-methyl-D-aspartate receptors containing the NR2B subunit. Characterization in vitro. J Pharmacol Exp Ther. 1997;283(3):1285-92.
68. Costa BM, Feng B, Tsintsadze TS, Morley RM, Irvine MW, Tsintsadze V, et al. N-methyl-D-aspartate (NMDA) receptor NR2 subunit selectivity of a series of novel piperazine-2,3-dicarboxylate derivatives: preferential blockade of extrasynaptic NMDA receptors in the rat hippocampal CA3-CA1 synapse. J Pharmacol Exp Ther. 2009;331(2):618-26.
69. Irvine MW, Costa BM, Volianskis A, Fang G, Ceolin L, Collingridge GL, et al. Coumarin-3-carboxylic acid derivatives as potentiators and inhibitors of recombinant and native N-methyl-D-aspartate receptors. Neurochem Int. 2012;61(4):593-600.
70. Anderson WW, Collingridge GL. Capabilities of the WinLTP data acquisition program extending beyond basic LTP experimental functions. J Neurosci Methods. 2007;162(1-2):346-56.
71. Auberson YP, Allgeier H, Bischoff S, Lingenhoehl K, Moretti R, Schmutz M. 5-Phosphonomethylquinoxalinediones as competitive NMDA receptor antagonists with a preference for the human 1A/2A, rather than 1A/2B receptor composition. Bioorg Med Chem Lett. 2002;12(7):1099-102.
72. Hernandez RV, Navarro MM, Rodriguez WA, Martinez JL, Jr., LeBaron RG. Differences in the magnitude of long-term potentiation produced by theta burst and high frequency stimulation protocols matched in stimulus number. Brain Res Brain Res Protoc. 2005;15(1):6-13.
73. Kouvaros S, Papatheodoropoulos C. Theta burst stimulation-induced LTP: Differences and similarities between the dorsal and ventral CA1 hippocampal synapses. Hippocampus. 2016;26(12):1542-59.
74. Martens U, Capito B, Wree A. Septotemporal distribution of [3H]MK-801, [3H]AMPA and [3H]Kainate binding sites in the rat hippocampus. Anat Embryol (Berl). 1998;198(3):195-204.
75. Pandis C, Sotiriou E, Kouvaras E, Asprodini E, Papatheodoropoulos C, Angelatou F. Differential expression of NMDA and AMPA receptor subunits in rat dorsal and ventral hippocampus. Neuroscience. 2006;140(1):163-75.
76. Papatheodoropoulos C. Striking differences in synaptic facilitation along the dorsoventral axis of the hippocampus. Neuroscience. 2015;301:454-70.
77. Maruki K, Izaki Y, Nomura M, Yamauchi T. Differences in paired-pulse facilitation and long-term potentiation between dorsal and ventral CA1 regions in anesthetized rats. Hippocampus. 2001;11(6):655-61.

78. Kouvaros S, Papatheodoropoulos C. Major dorsoventral differences in the modulation of the local CA1 hippocampal network by NMDA, mGlu5, adenosine A2A and cannabinoid CB1 receptors. Neuroscience. 2016;317:47-64.
79. Babiec WE, Jami SA, Guglietta R, Chen PB, O'Dell TJ. Differential Regulation of NMDA Receptor-Mediated Transmission by SK Channels Underlies Dorsal-Ventral Differences in Dynamics of Schaffer Collateral Synaptic Function. J Neurosci. 2017;37(7):1950-64.
80. Kleschevnikov AM, Sokolov MV, Kuhnt U, Dawe GS, Stephenson JD, Voronin LL. Changes in paired-pulse facilitation correlate with induction of long-term potentiation in area CA1 of rat hippocampal slices. Neuroscience. 1997;76(3):829-43.
81. Hansen KB, Ogden KK, Yuan H, Traynelis SF. Distinct functional and pharmacological properties of Triheteromeric GluN1/GluN2A/GluN2B NMDA receptors. Neuron. 2014;81(5):1084-96.
82. Yi F, Bhattacharya S, Thompson CM, Traynelis SF, Hansen KB. Functional and pharmacological properties of triheteromeric GluN1/2B/2D NMDA receptors. J Physiol. 2019;597(22):5495-514.

Fig.1 Ventral STP and LTP; Ingram R et al 2024

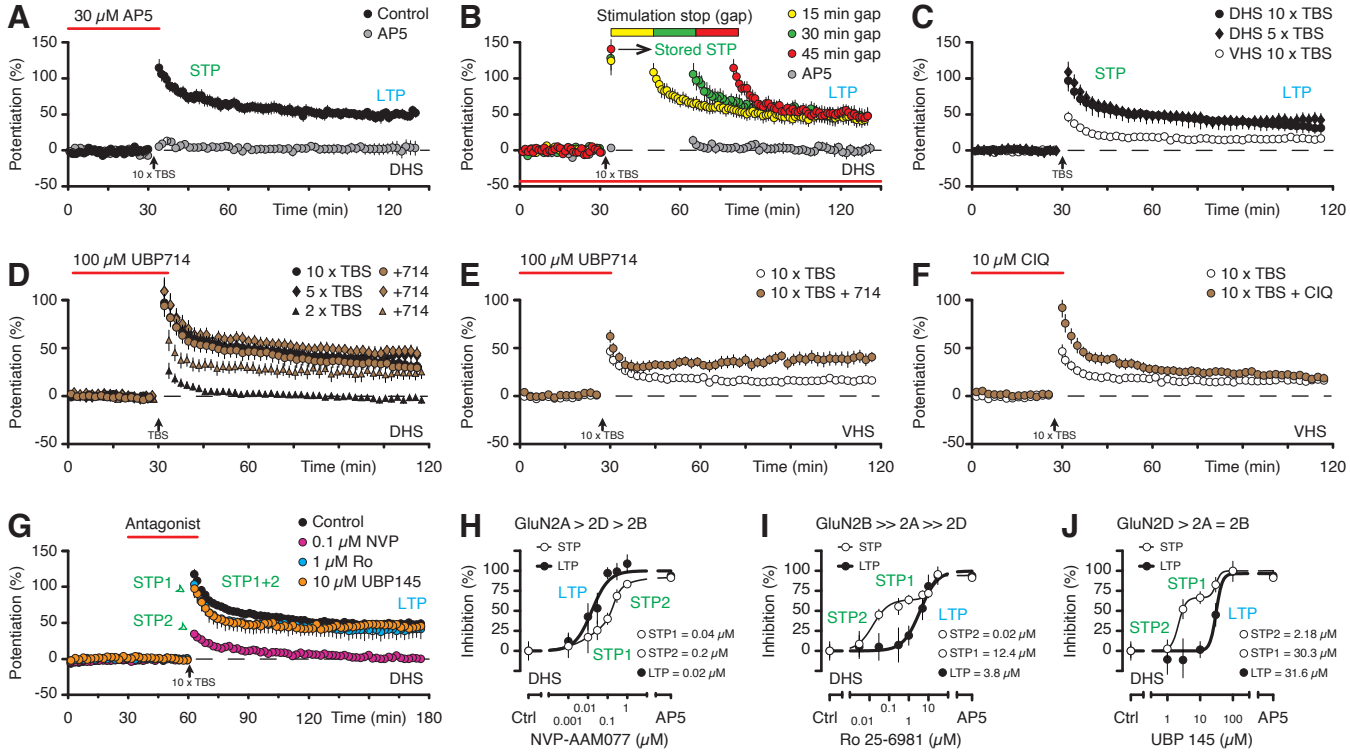

Fig.2 Ventral STP and LTP; Ingram R et al 2024

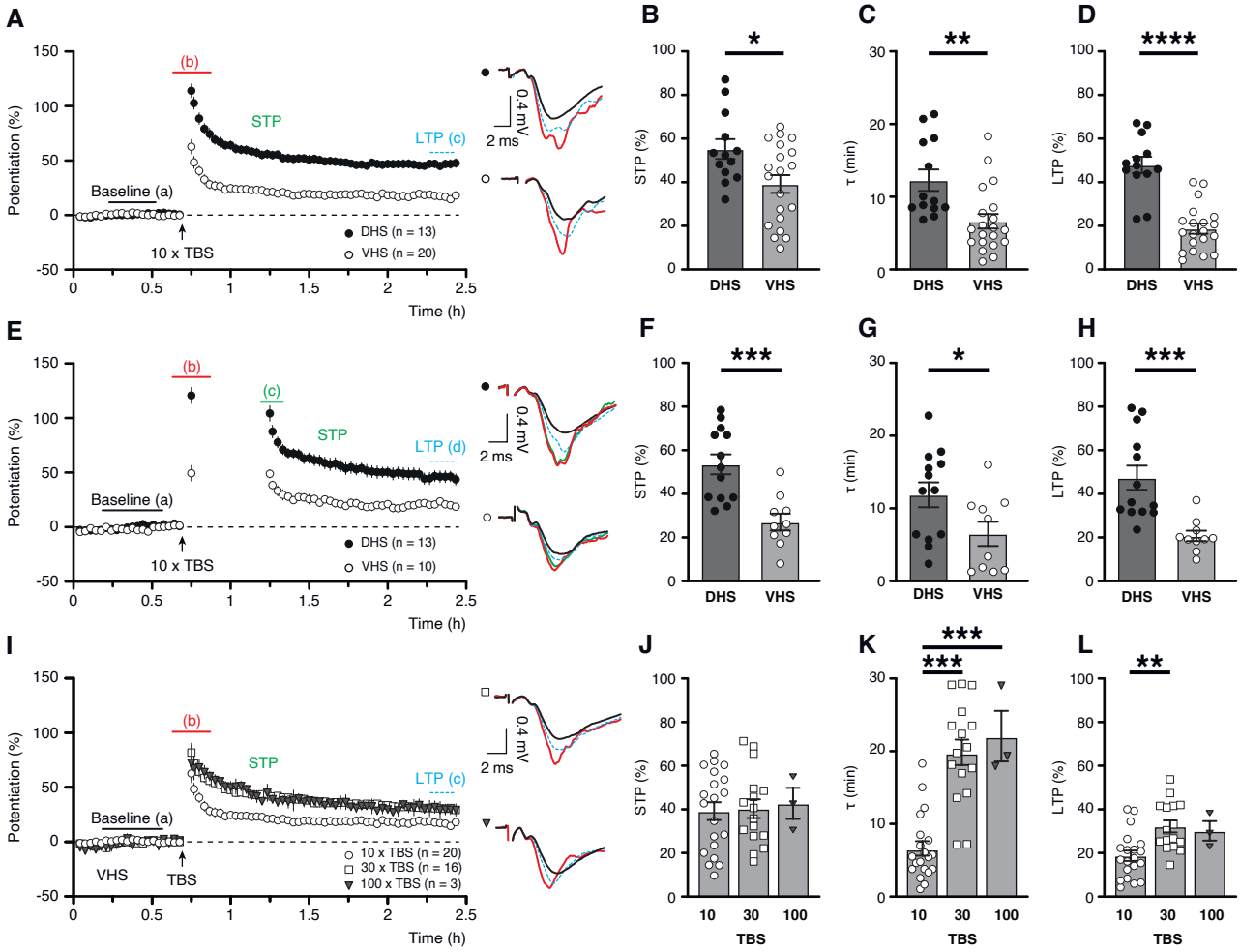

Fig.3 Ventral STP and LTP; Ingram R et al 2024

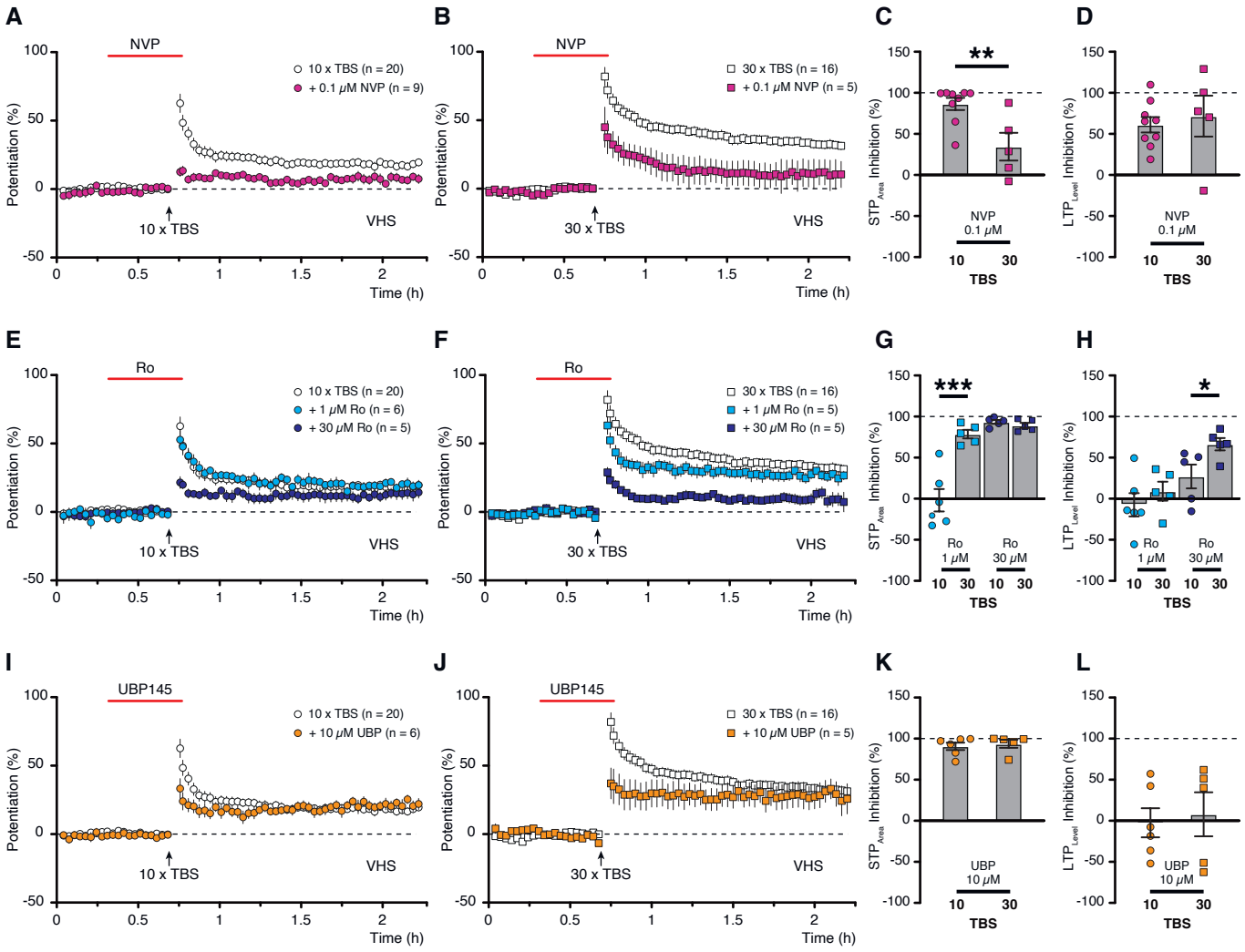

Fig.4 Ventral STP and LTP; Ingram R et al 2024

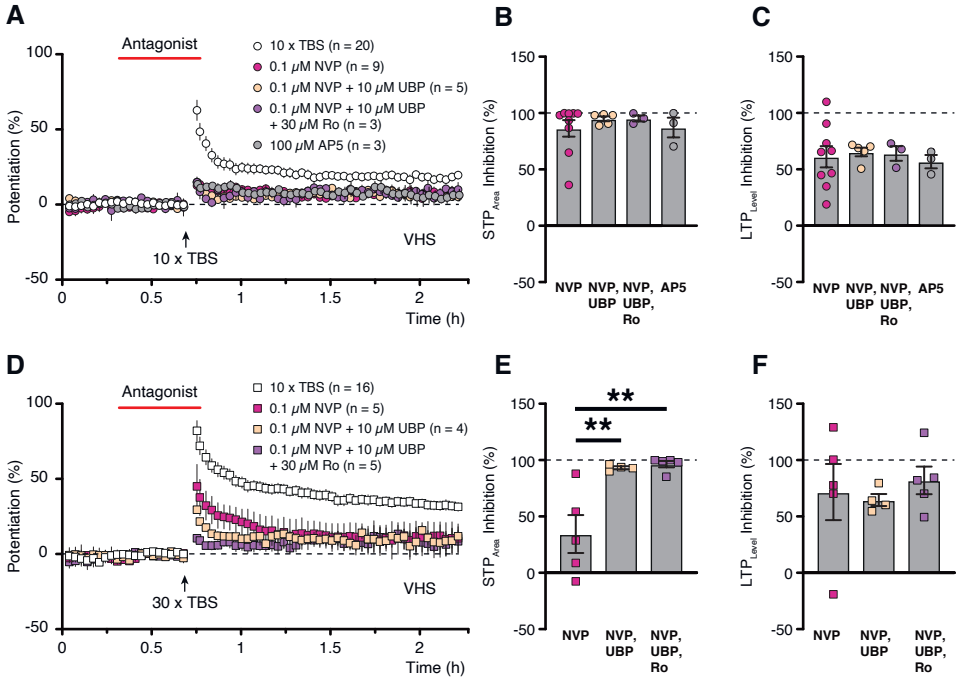

Fig.5 Ventral STP and LTP; Ingram R et al 2024

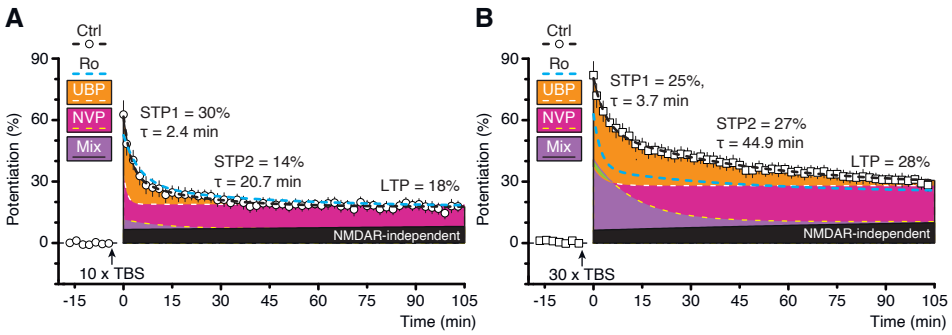

Table 1. Pharmacological characterisation of NMDAR-subunit preferring compounds.

Subunits / Compounds	GluN2A (recombinant)	GluN2B (recombinant)	GluN2C (recombinant)	GluN2D (recombinant)	NMDARs (neurons)
D-AP5^{CA}	0.28$^{\#}$ / 1.06†	0.46$^{\#}$ / 2.68†	1.64$^{\#}$	3.71$^{\#}$ / 44.9†	0.6†
CIQ^{PAM}	> 10‡	>10‡	2.7‡	2.8‡	130§
NVP-AAM077^{CA}	0.0054$^{\#}$ / 0.048†	0.067$^{\#}$ / 0.6†	0.012$^{\#}$	0.037$^{\#}$ / 0.1†	0.033†
Ro 25-6981^{NAM}	52 to 250†	0.009 to 0.057†	unknown	no inhibition	1.22†
UBP145^{CA}	11.5$^{\#}$ / 16†	8.0$^{\#}$ / 13†	2.8$^{\#}$	1.19$^{\#}$ / 1.3†	11.5†
UBP714^{PAM}	17§	14§	unknown	4.4§	17§

NMDAR compounds that are discussed in current study. Symbols represent: $^{\#}$ K_i values, † IC_{50} values, ‡ EC_{50} values, § % potentiation above control levels. All data are given in µM. CA – competitive antagonists, PAM – positive allosteric modulator, NAM – negative allosteric modulator. D-AP5 data from (1, 2) [62, 64]. CIQ data from (3) [65], please note that potentiation of native NMDARs is for the subthalamic neurons and no potentiation was seen for the CA1 pyramidal cells. NVP-AAM077 data from (1, 4) [62, 66], please note that in (4) [66] NVP is referred to as PEAQX. Ro 25-6981 data from (1, 5) [62, 67]. UBP145 data from (1, 6) [62,68]. UBP714 data from (7) [69].

References for the table () in cyan should be deleted for the final production, references in yellow [] correspond to reference order in the main document:

1. Volianskis A, Bannister N, Collett VJ, Irvine MW, Monaghan DT, Fitzjohn SM, et al. Different NMDA receptor subtypes mediate induction of long-term potentiation and two forms of short-term potentiation at CA1 synapses in rat hippocampus in vitro. J Physiol. 2013;591(4):955-72.
2. Buller AL, Monaghan DT. Pharmacological heterogeneity of NMDA receptors: characterization of NR1a/NR2D heteromers expressed in Xenopus oocytes. Eur J Pharmacol. 1997;320(1):87-94.
3. Mullasseril P, Hansen KB, Vance KM, Ogden KK, Yuan H, Kurtkaya NL, et al. A subunit-selective potentiator of NR2C- and NR2D-containing NMDA receptors. Nat Commun. 2010;1:90.
4. Feng B, Tse HW, Skifter DA, Morley R, Jane DE, Monaghan DT. Structure-activity analysis of a novel NR2C/NR2D-preferring NMDA receptor antagonist: 1-(phenanthrene-2-carbonyl) piperazine-2,3-dicarboxylic acid. Br J Pharmacol. 2004;141(3):508-16.
5. Fischer G, Mutel V, Trube G, Malherbe P, Kew JN, Mohacsi E, et al. Ro 25-6981, a highly potent and selective blocker of N-methyl-D-aspartate receptors containing the NR2B subunit. Characterization in vitro. J Pharmacol Exp Ther. 1997;283(3):1285-92.
6. Costa BM, Feng B, Tsintsadze TS, Morley RM, Irvine MW, Tsintsadze V, et al. N-methyl-D-aspartate (NMDA) receptor NR2 subunit selectivity of a series of novel piperazine-2,3-dicarboxylate derivatives: preferential blockade of extrasynaptic NMDA receptors in the rat hippocampal CA3-CA1 synapse. J Pharmacol Exp Ther. 2009;331(2):618-26.
7. Irvine MW, Costa BM, Volianskis A, Fang G, Ceolin L, Collingridge GL, et al. Coumarin-3-carboxylic acid derivatives as potentiators and inhibitors of recombinant and native N-methyl-D-aspartate receptors. Neurochem Int. 2012;61(4):593-600.